Colloids and Interface Science Communications 1 (2014) 18–22

Contents lists available at ScienceDirect

Colloids and Interface Science Communications

journal homepage: www.elsevier.com/locate/colcom

Rapid Communication

Influence of the Disjoining Pressure on the Equilibrium Interfacial Profile in Transition Zone Between a Thin Film and a Capillary Meniscus

I.V. Kuchin [a], O.K. Matar [b], R.V. Craster [c], V.M. Starov [a,*]

[a] Department of Chemical Engineering, Loughborough University, Loughborough LE113TU, UK
[b] Department of Chemical Engineering, Imperial College London, South Kensington Campus, London SW72AZ, UK
[c] Department of Mathematics, Imperial College London, South Kensington Campus, London SW72AZ, UK

ARTICLE INFO

Article history:
Received 25 March 2014
Accepted 2 June 2014
Available online 24 June 2014

Keywords:
disjoining/conjoining pressure
equilibrium meniscus
wetting phenomena
contact angle
DLVO theory
electrostatic interaction
Poisson–Boltzmann equation
van der Waals interaction
augmented Young-Laplace equation
transition zone

ABSTRACT

The behaviour of liquid layers on solid substrates depends on a number of factors, the most important of which is the action of surface forces in the vicinity of the three phase contact line. The equilibrium interfacial (gas/liquid) profile in the transition zone between the thin flat film and the spherical part of a meniscus is determined by the combined action of the disjoining/conjoining and capillary pressures. The disjoining/conjoining pressure is considered to include the electrostatic, van der Waals and structural components. The Poisson–Boltzmann equation is also solved with various boundary conditions to calculate the electrostatic component of the disjoining/conjoining pressure. Wetting conditions are considered and the interfacial profile is determined for various parameters governing the surface interactions, as well as the ratio between the disjoining/conjoining and capillary pressures.

© 2015 The Authors. Published by Elsevier Inc. Open access under CC BY license. (http://creativecommons.org/licenses/by/4.0/).

1. Introduction

DCP[1] is a manifestation of the surface forces acting on thin liquid layers and this concept was introduced, and successfully investigated, in the pioneering works of Derjaguin [1,2]. The well-known DLVO (Derjaguin–Landau–Verwey–Overbeek) theory of colloidal stability is based on DCP acting between colloidal particles/droplets [1]. DCP also acts in the vicinity of the three-phase contact line in the case of wetting/spreading [3], and for historical reasons, the action of DCP under these conditions has received less attention. However, there are notable examples where the effect of surface forces on wetting and spreading phenomena of liquids on solid substrates are considered (see [4–7] and references therein).

Flat wetting films on solid substrates exist because the DCP inside the liquid film is balanced by CP[2] in the neighbouring meniscus or droplet. Within the spherical part of the meniscus or droplet, the separation between the liquid–vapour and solid–liquid interfaces is high and the DCP is negligible. Hence, the shape of the meniscus or droplet is determined by the action of CP only [3]. Therefore, a transition zone must exist between the bulk meniscus or droplet and the flat film wherein DCP and CP act simultaneously [3,5,7]. Since measurements of equilibrium/hysteresis contact angles and surface curvature of bulk liquids are carried out outside the transition zone, its size and profile are of interest. The latter provide information on the DCP-isotherm for thin liquid films on a solid substrate. The transition profile of the meniscus was calculated in [3] for the case of complete wetting. The primary aim of this article is to determine the shape of the transition zone for various types of the DCP-isotherm. The exact numerical solutions for PW conditions and for complicated forms of the DCP-isotherm were obtained for the first time.

2. Model Description

2.1. Model Assumptions

The transition zone *II* (Fig. 1) under equilibrium conditions is located between a two dimensional capillary meniscus (*I*) and a flat wetting film (*II*). A rectangular coordinate system, (x_1, x_2) is used, in which x_1 and x_2 are the lateral and normal coordinates, respectively. The width of the capillary, $2H$, is assumed to be much larger than the thickness of the equilibrium flat film, h_e. In the case of CW[3] (see Fig. 1,*a*), the

* Corresponding author. Tel.: +44 1509 222508; fax: +44 1509 223923.
E-mail address: V.M.Starov@lboro.ac.uk (V.M. Starov).

[1] DCP — disjoining/conjoining pressure.
[2] CP — capillary pressure.
[3] CW — complete wetting.

http://dx.doi.org/10.1016/j.colcom.2014.06.002
2215-0382/© 2015 The Authors. Published by Elsevier Inc. Open access under CC BY license. (http://creativecommons.org/licenses/by/4.0/).

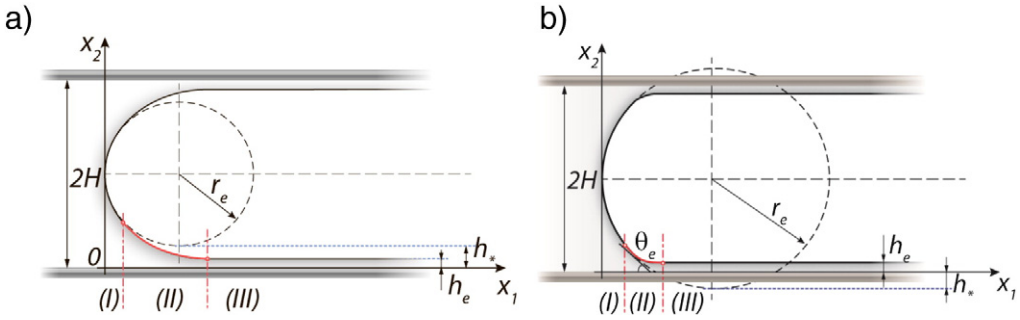

Fig. 1. Schematic presentation of a capillary meniscus under CW (*a*) and PW (*b*) conditions. *I* — spherical capillary meniscus; *II* — transition zone; *III* — flat wetting films. *a*) $\theta_e = 0$, $r_e < H$, $h^* = H - r_e > 0$; *b*) $\theta_e > 0$, $r_e > H$, $h^* = H - r_e < 0$.

continuation of the spherical meniscus (broken line) of radius r_e does not intersect either the solid walls of the capillary or the thin liquid film of thickness h_e. The case of PW[4] is shown in Fig. 1,*b*; the continuation of the spherical meniscus intersects the boundary at the contact angle θ_e.

Under equilibrium conditions, there is no flow, and zero ion fluxes. The surface tension is assumed to be constant, which is valid in the absence of surfactants (and thermal gradients) [8].

2.2. Expression for the DCP Isotherm

The full DCP is a sum of electrostatic, van der Waals and structural components:

$$\Pi = \Pi_E + \Pi_W + \Pi_S. \tag{1}$$

The van der Waals component [1] is given by

$$\Pi_w = \frac{A}{6\pi h^3}. \tag{2}$$

Here $A = -A_H$, A_H is the Hamaker constant; and h is a thickness of the liquid film. The influence of the structural component, Π_S, is discussed later (see Effect of the structural component section). An example of the graphic dependences of the DCP components will be given in Fig. 5,a.

To derive an expression for the electrostatic component, Π_E, the Poisson–Boltzmann equation in the small-slope approximation, $h'^2 \ll 1$, where the prime denotes differentiation with respect to x_1, is used:

$$\frac{\partial^2 \varphi}{\partial x_2^2} = \frac{F^2 c_0}{RT\varepsilon\varepsilon_0}(\exp(\varphi) - \exp(-\varphi)) \tag{3}$$

where $\varphi = \Phi F/(RT)$ is a dimensionless potential in which the dimensional potential, Φ, is scaled on F/RT, wherein F is the Faraday constant, R is the gas constant, and T denotes the temperature, respectively; c_0 is the molar electrolyte concentration; ε and ε_0 are the dielectric constants of water and vacuum, respectively.

In the case of equilibrium, the momentum equations in the x_i directions ($i = 1,2$) are expressed by the equations of electrohydrodynamics [9,10]:

$$-\frac{\partial p}{\partial x_i} - q\frac{RT}{F}\frac{\partial \varphi}{\partial x_i} = 0 \tag{4}$$

where $q = Fc_0(\exp(-\varphi) - \exp(\varphi))$ is a volume charge density; and p is the pressure in the liquid.

[4] PW — partial wetting.

Eqs. (3) and (4) are used in the normal stress balance at gas–liquid interface in the transition zone [3]:

$$-p - \frac{1}{2}\varepsilon\varepsilon_0 E^2 + \varepsilon\varepsilon_0 E_2^2 = \frac{d}{dx_1}\frac{\gamma h'}{\sqrt{1+h'^2}}, \quad x_2 = h$$

where $E_i = -\frac{RT}{F}\frac{\partial \varphi}{\partial x_i}$ is the electric field; γ is the surface tension of solution.

Taking into account in the last equation that $\frac{\partial}{\partial x_1} << \frac{\partial}{\partial x_2}$, the following expression for the electrostatic component in the case of the small-slope profiles is obtained:

$$\Pi_E = RTc_0(\exp(\varphi) + \exp(-\varphi)) - 2RTc_0 - \frac{(RT)^2\varepsilon\varepsilon_0}{2F^2}\left(\frac{\partial \varphi}{\partial x_2}\right)^2. \tag{5}$$

The following boundary conditions are used here: $\Pi(h \to \infty) = 0$ and $\varphi(h \to \infty) = 0$, which correspond to the decay conditions for the DCP and the electric potential at long distances. The detailed description of the derivation of Eq. (5) and an analysis of the results for CW conditions are given in [11].

Eq. (5) coincides with Derjaguin's expression [1] for flat films. However, there is a substantial distinction of the expression (5) from that deduced in [1]: Eq. (5) is valid for non-flat thin liquid films in the case of small-slope approximation.

Two types of boundary conditions for Eq. (3) are used below to find the distribution of $\varphi(x_2)$ and $\partial\varphi/\partial x_2$ across the liquid film:

(1) constant surface electrical potentials on both liquid–solid and liquid–vapour interfaces: φ_s, φ_h = const;
(2) constant surface charge densities σ_s, σ_h = const.

The situations when $\varphi_s \neq \varphi_h$ or $\sigma_s \neq \sigma_h$ are rather common and will be studied below.

The equilibrium interfacial profile under the action of the surface forces is described by the augmented Young–Laplace equation [1,3]:

$$\frac{\gamma h''}{(1+h'^2)^{3/2}} + \Pi(h) = P_e. \tag{6}$$

Here P_e is the excess pressure equal to the capillary pressure for the spherical meniscus, $P_e = \gamma/(H - h^*)$.

Eq. (6) representing the normal stress balance, is solved for the case γ = const. The calculation results are discussed in the Equilibrium interfacial profile in the transition zone section. For the systems with the surface tension gradients, the significant tangential stress along

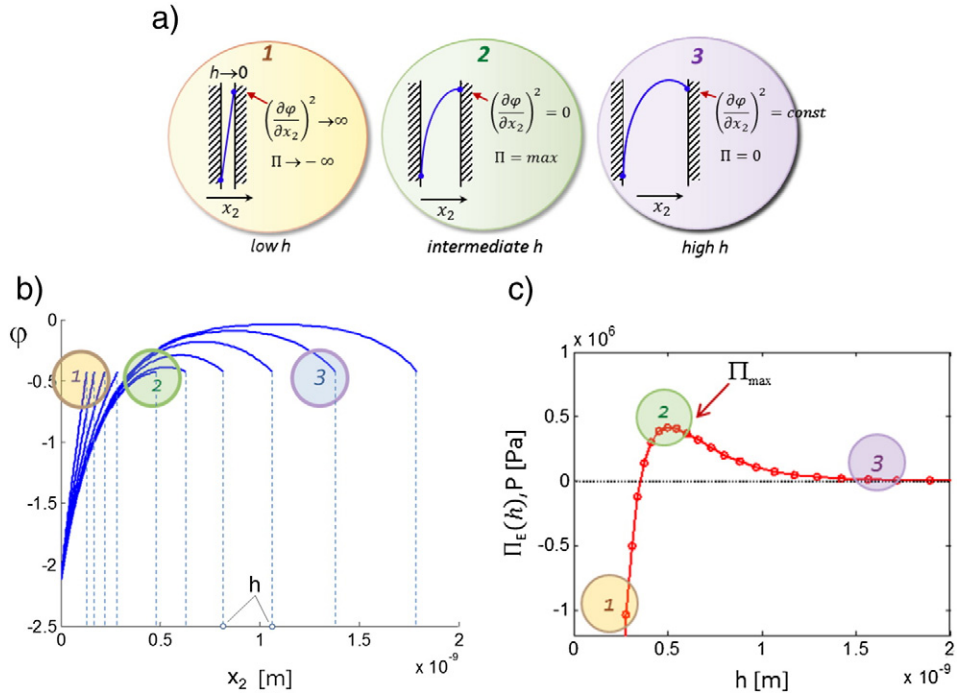

Fig. 2. Analysis of the complex character of the DCP isotherm for the case $\varphi_{h,s} =$ const; $\varphi_s = -2.12$; $\varphi_h = -0.42$. Three types of electric potential profiles (*a*); the potential distributions at *h* variation (*b*); the calculated DCP isotherm (*c*).

the interface can arise, and the tangential stress balance must also be taken into account.

2.3. Results for the DCP Calculation

An aqueous solution of a strong, univalent electrolyte, NaCl, was chosen for the calculations: temperature $T = 293$ [K]; bulk NaCl concentration $c_0 = 1$ [mole/m^3]; surface tension of solution $\gamma = 72.7 \times 10^{-3}$ [N/m].

Let us first consider the case in which both φ_s and φ_h are constant but $\varphi_s \neq \varphi_h$ for which the results are presented in Fig. 2. The distribution of potentials is asymmetric (Fig. 2,*b*), and since both φ_s and φ_h are constant, the surface charges $\sigma_{h,s}$ are not, as demonstrated by the varying values of the potential slopes at the boundaries in Fig. 2,*b*. The isotherm Π_E has a maximum in this case (Fig. 2,*c*): at high separations, repulsion prevails, whereas at small distances attraction is observed. Since the electric potentials on the boundaries are constant, the DCP can change only due to the variation of the Maxwell part (corresponding to the last term) in Eq. (5).

For low *h* values (region 1 in Fig. 2), the gradient $\partial\varphi/\partial x_2$ tends to infinity because for the case $\varphi_{h,s} =$ constant, the difference $\Delta\varphi = \varphi_h - \varphi_s$ is also constant at $x_2 \to 0$ (Fig. 2,*a*, case 1). According to Eq. (5), this results in $\Pi \to -\infty$ at low separations *h* between the surfaces. In region 2, of the intermediate values of *h*, the gradient $\partial\varphi/\partial x_2$ decreases and at a certain *h* it becomes equal to zero. Under these conditions, the Maxwell part of the DCP is absent and the DCP takes its maximum value Π_{max}, which is equal to the excess osmotic pressure in the film. Finally, at large distances, *h*, the gradient $\partial\varphi/\partial x_2$ becomes negative, reaches its limiting value, and does not depend anymore on the increase of *h* (Fig. 2, region 3). In this region, the surfaces are non-interacting, the Maxwell part for them becomes constant and equals to the excess osmotic pressure, Π_{max}.

In view of the above, the maximum of the DCP isotherm is related to the sign change of the gradient $\partial\varphi/\partial x_2$, which is proportional to the surface electric charge σ: one of the surfaces changes its charge sign in response to the variation in *h*. A physical explanation for this behaviour could be the phenomenon of a surface charge reversal or overcharging [12,13]. However, the DCP changes its sign not at the point of overcharging, but at the point where the Maxwell part of the DCP in Eq. (5) becomes equal to the osmotic part.

A similar analysis can be made for the case $\sigma_{h,s} =$ constant; the minimum on the DCP isotherm is explained here by the variation of the osmotic contribution of the DCP with the Maxwell part remaining constant.

3. Equilibrium Interfacial Profile in the Transition Zone

3.1. Equations for the Equilibrium Interfacial Profile

The equilibrium interfacial profile is found from the following equation obtained by integration of Eq. (6) using the boundary condition $h'(h \to H) = -\infty$:

$$\frac{dh}{dx_1} = -\sqrt{-1 + \frac{\gamma^2}{\left[\frac{\gamma}{r_e}(H-h) - \int_h^\infty \Pi dh\right]^2}}. \tag{7}$$

Here $\gamma/r_e = P_e$ in which $r_e = H - h^*$ is the radius of the equilibrium meniscus (see Fig. 1 for definition of h^*), and the upper limit of integration was replaced by infinity because the DCP vanishes at distances compared with a capillary width scale.

The solution of Eq. (7) must satisfy the boundary conditions in the flat film region: $h(\infty) = h_e$; $h'(\infty) = 0$. Substitution of these conditions into Eq. (7) gives the following relation:

$$\gamma = \frac{\gamma}{r_e}(H - h_e) - \int_{h_e}^{\infty} \Pi dh. \tag{8}$$

If the contact angle θ_e is determined by the intersection of the spherical meniscus with the flat film, the equilibrium contact angle from

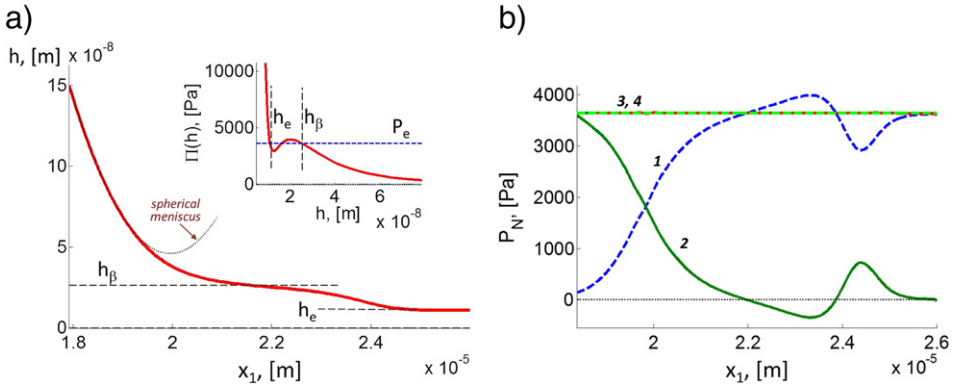

Fig. 3. The equilibrium interfacial profile (a) and normal stress components distribution (b) under CW conditions: $A = 3.36 \times 10^{-18}$ J; $H = 2.0 \times 10^{-5}$ m; $\theta_e = 0$. In panel (b): *1* — DCP; *2* — local capillary pressure due to the profile curvature, γK; *3* — total pressure, $\gamma K + \Pi$; *4* —excess pressure P_e (CP for a spherical meniscus, γ/r_e).

Eq. (8) is:

$$\cos\theta_e = \frac{H - h_e}{r_e} = 1 + \frac{1}{\gamma}\int_{h_e}^{\infty} \Pi dh. \tag{9}$$

The latter expression was firstly obtained by Derjaguin and Frumkin from the Gibbs adsorption equation [14,15]. The dependence $\Pi(h)$ in the above equations can be calculated using Eqs. (1), (2) and (5). Under PW conditions $\cos\theta_e < 1$; in CW case $\cos\theta_e > 1$. The last condition has no mathematical meaning, it simply means that $H - h_e > r_e$.

Calculations using Eq. (7) require knowledge of two unknown values: the radius of the equilibrium meniscus, $r_e = H - h^*$, and the thickness of the equilibrium flat film, h_e. The normal stress balance according to Eq. (6) for the flat film (h', $h'' = 0$) in combination with Eqs. (2) and (5), solved simultaneously with Eq. (8), gives a system of two equations with two unknown values h_e and h^*:

$$\begin{cases} RTc_0\left(\exp(\varphi) + \exp(-\varphi)\right)_{x_2=h_e} - \dfrac{(RT)^2\varepsilon\varepsilon_0}{2F^2}\left(\dfrac{\partial\varphi}{\partial x_2}\right)^2_{x_2=h_e} - 2RTc_0 - \dfrac{A}{6\pi h_e^3} = \dfrac{\gamma}{H-h^*} \\ \dfrac{h^*}{H} = 1 - \dfrac{1 - h_e/H}{1 + \dfrac{1}{\gamma}\displaystyle\int_{h_e}^{\infty}\Pi dh}. \end{cases} \tag{10}$$

As was mentioned above, the structural component of Π is not used in Eq. (10). After the values h^* and h_e are found, the interface profile in the transition zone is calculated using Eq. (7).

3.2. Results of the Equilibrium Interfacial Profile Calculation

The electrostatic component of the DCP was calculated for the case of constant surface charge density $\sigma_{s,h} = \text{const}$, with $\sigma_s = -150$ mC and $\sigma_h = 150$ mC at the boundaries. The van der Waals component of the DCP was also included in calculations. The effect of the structural component is considered in the Effect of the structural component section.

As shown in the inset to Fig. 3,*a*, there are three points of intersection of the DCP with P_e line: the points h_e and h_β correspond to the stable and metastable equilibrium states. The CW conditions are observed; this follows from the form of the DCP isotherm: the integral in Eq. (9) is positive. There is a small-slope plateau in the convex part corresponding to the metastable state h_β (Fig. 3,*a*).

Fig. 3,*b* shows that DCP (curve 1) has a maximum value exceeding the excess pressure P_e (line 4) in the vicinity of point $x_1 \approx 2.3 \times 10^{-5}$ m, i.e. in the interval between h_u and h_β. Since the total pressure (i.e. the sum of DCP and the local CP) must be constant, the magnitude γK becomes negative in this interval (curve 2). As a result, the profile curvature K changes its sign and the convex part appears in the interface profile (Fig. 3,*a*). It is obvious that the necessary condition for the presence of the convex part is the triple intersection of the DCP with P_e, i.e. the multiplicity of the equilibrium states [1].

In PW case the condition $\cos\theta_e < 1$ is valid, hence according to Eq. (9) the condition $\int_{h_e}^{\infty}\Pi dh < 0$ is satisfied and the DCP-isotherm includes a negative (attractive) part. The interface profile including the convex part for the case of PW conditions is presented in Fig. 4, for which $\theta_e = 0.9°$. There are three intersection points in the inset, hence the convex part is

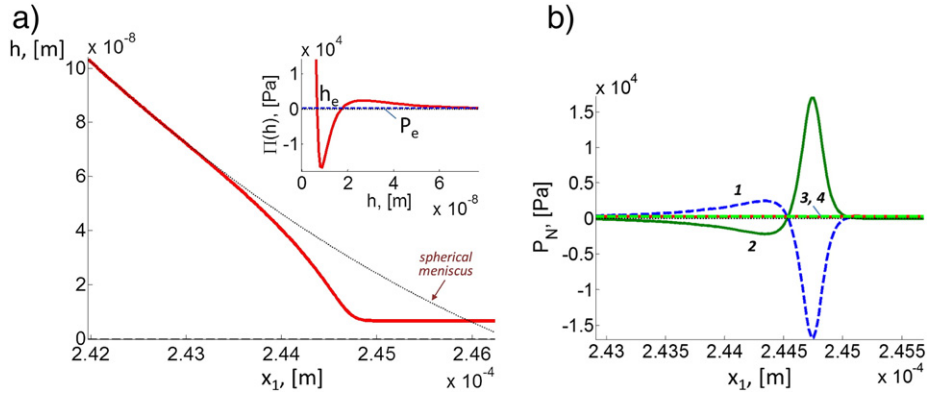

Fig. 4. The equilibrium interfacial profile (a) and normal stress components (b) under the PW conditions: $A = 3.0 \times 10^{-18}$ J; $H = 2.5 \times 10^{-4}$ m; $\theta_e = 0.9°$. The curves definitions in panel (b) correspond to Fig. 3.

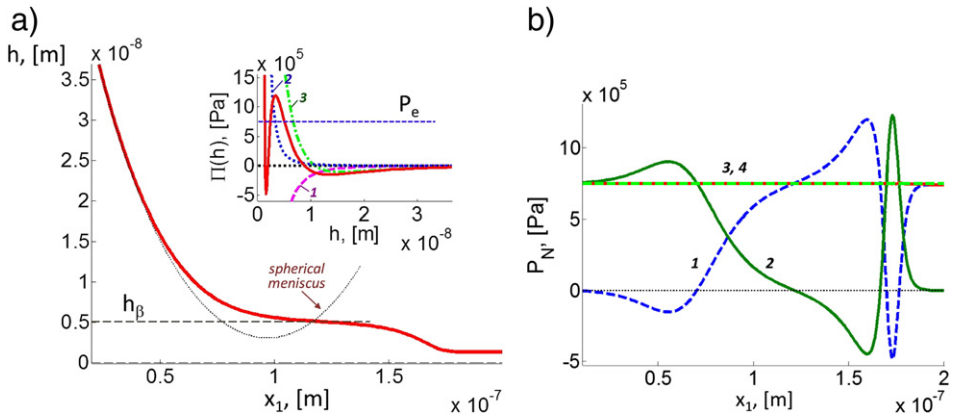

Fig. 5. The effect of the structural interaction on the equilibrium interfacial profile (a) and on the stress component distribution (b). CW conditions, $\theta_e = 0$. $A = 5.05 \times 10^{-19}$ J; $K_1 = 1.5 \times 10^7$ Pa; $K_2 = -5.0 \times 10^5$ Pa; $\lambda_1 = 2.5 \times 10^{-9}$ m; $\lambda_2 = 12 \times 10^{-9}$ m; $H = 1.0 \times 10^{-7}$ m. Inset in panel (a): *1,2,3* — electrostatic, van der Waals and structural components, respectively. Panel (b): the curve definitions correspond to Fig. 3.

observed on the interface profile. Around the point $x_1 \approx 2.445 \times 10^{-4}$ m, the DCP (curve 1 in Fig. 4,*b*) has a maximum where $\Pi > P_e$ (line 4). As a result, $K < 0$ here (curve 2) which corresponds to the convex part in Fig. 4,*a*; the convex is most pronounced at low values of the contact angle for the case of PW conditions.

3.3. Effect of the Structural Component

In this section, the structural component of the DCP is included in calculation in addition to the electrostatic and van der Waals components. The structural component Π_S of the DCP was calculated using the following dependence [16]:

$$\Pi_S = K_1 \exp(-h/\lambda_1) + K_2 \exp(-h/\lambda_2),$$

where K_1, K_2 and λ_1, λ_2 are the parameters related to the magnitude and the characteristic length of the structural forces. The indexes 1 and 2 correspond to the short-range and long-range structural interactions, respectively. The structural component can arise due to the changes in the orientation structure of polar liquid near the surface [1,16].

A long-range structural attraction causes an additional secondary minimum in the DCP isotherms (Fig. 5,*a*, inset). This attraction (the negative values of the DCP shown by curve 1 in Fig. 5,*b*) is the reason that the values of the profile curvature (curve 2, Fig. 5,*b*) exceed the curvature of the spherical meniscus (line 4, Fig. 5,*b*). As a result, the interface profile is curved more sharply than the spherical meniscus is, and the convex part of the interface is located as shown in Fig. 5,*a*. This behaviour takes place for both CW and PW conditions. It should be noted that the convex part is observed in the case of the equilibrium states multiplicity only as it was mentioned above.

4. Conclusion

Calculation of the equilibrium interfacial profile inside the transition zone between a spherical meniscus and a thin liquid film has been carried out; this calculation has also yielded the equilibrium contact angle, the disjoining/conjoining pressure (DCP) isotherms, and the distribution of electric potential and charge in the liquid phase. The precise numerical integration of the augmented Young–Laplace equation was performed for the first time for various types of the DCP isotherm. The obtained results indicate that the form of the isotherm has a significant effect on the shape of the equilibrium interfacial profile in the transition zone: the convex part in the interface profile depends on the equilibrium states between the DCP and excess pressure. For complete wetting conditions, the convex part of the interface is usually observed in front of the spherical meniscus, whereas for partial wetting, it is located behind it. Inclusion of the van der Waals component in the DCP leads to an increase in the latter, and, as a result, a growth of the flat film thickness and a decrease of the meniscus radius. The structural component leads to the interface profile shape with a convex part in front of the meniscus for both complete and partial wetting conditions.

Acknowledgements

This research was supported by EPSRC grant EP/J010502/1. V. Starov's research was also supported by CoWet Project, (607861) EU.

References

[1] B.V. Derjaguin, N.V. Churaev, V.M. Muller, Surface Forces, Springer, 1987.
[2] B.V. Derjaguin, Colloid J. 17 (3) (1955) 191–197.
[3] V.M. Starov, M.G. Velarde, C.J. Radke, Wetting and Spreading Dynamics, Taylor and Francis/CRC, New York, 2007.
[4] N.V. Churaev, V.D. Sobolev, Adv. Colloid Interf. Sci. 61 (1995) 1–16.
[5] P.A. Kralchevsky, I.B. Ivanov, Chem. Phys. Lett. 121 (1985) 111–115.
[6] I.B. Ivanov, B.V. Toshev, Colloid Polym. Sci. 253 (1975) 593–599.
[7] B.V. Derjaguin, V.M. Starov, N.V. Churaev, J. Colloid Interface Sci. 89 (1982) 16–24.
[8] G. Karapetsas, R.V. Craster, O.K. Matar, J. Fluid Mech. 670 (2011) 5–37.
[9] A.I. Zhakin, Phys. Usp. 55 (5) (2012) 465–488.
[10] Electrohydrodynamics, in: A. Castellanos (Ed.), Springer, 1998.
[11] I.V. Kuchin, O.K. Matar, R.V. Craster, V.M. Starov, Soft Matter (2014) (accepted for publication).
[12] J. Lyklema, Colloids Surf. A 291 (2006) 3–12.
[13] A. Martin-Molina, C. Rodriguez-Beas, R. Hidalgo-Álvarez, M. Quesada-Pérez, J. Phys. Chem. B 113 (2009) 6834.
[14] A.N. Frumkin, Zh. Fiz. Khim. 12 (1938) 337.
[15] B.V. Derjaguin, Zh. Fiz. Khim. 14 (1940) 137.
[16] N.V. Churaev, V.D. Sobolev, Adv. Colloid Interf. Sci. 134–135 (2007) 15–23.